Design, modeling, and manufacturing of functionally graded sandwich panels

Master Research Project

Author: Josep Oriol Riu Martinez

Advisor: Lorenzo Valdevit

Master of Science in Mechanical and Aerospace Engineering

The Henry Samueli School of Engineering

University of California, Irvine

November 30, 2016

Contents

1 Introduction

Sandwich materials are structures made of two stiff skins and a softer lightweight core in between them. The function of the core is to separate the face sheets without significantly increasing the weight, thus increasing the moment of inertia of the structure. This makes sandwich structures convenient and efficient to resist bending and buckling loads while keeping a light weight, especially for applications where the weight is a critical factor (such as naval, aerospace, the transport industry and sporting equipment). [1, 2, 3]

For applications requiring resistance to impact loading (such as ship hulls, armors, helmets...) sandwich materials have good capabilities in absorbing energy [4]. The face sheets are designed to resist penetration/fracture, while the core is comprised of a material able to deform at a controlled level of stress providing isolation and damping of vibrations. [5]

The possible modes of failure of a sandwich panel are: face yielding or fracture, face and core indentation, face wrinkling (local buckling of the face sheets), core failure (usually in shear), and failure in the bonding between the core and the face sheets. This last one is the most difficult to analyze because delamination is affected by the nature of the interface between the two materials and also depends on the kind of adhesive being used. Oftentimes the adhesive is stronger than the core itself, so the bond is not a problem unless an interfacial crack appears which may propagate and separate the structure. [2, 5]

Functionally graded materials (FGM) are characterized by the gradual variation of the composition over the volume, which implies a gradual variation of the mechanical properties. This concept can be used in a sandwich structure in order to enhance its performance and better tailor its properties [6, 7]. More precisely, the concept of FGM can be used in sandwich structures to improve the interface between the face sheets and the core, making it a smooth transition between materials, in order to mitigate the bonding failure and delamination at the interface [8].

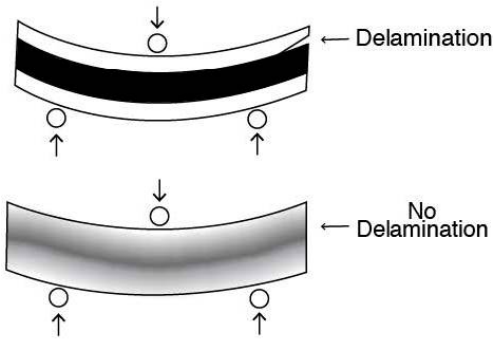

Figure 1: Difference between a classic sandwich and a functionally graded sandwich loaded in bending.

Multi-material Additive Manufacturing has created the opportunity of building structures that contain different materials with very dissimilar mechanical properties integrated in the same body. This technology can allow manufacturing complex parts while controlling at a microscopic scale the local composition of the material being printed, which can be used to generate functionally graded materials. In this project, the device used is a Stratasys Objet260 Connex3 which can print blending up to three different base materials in the same part, although only a two material gradation has been studied.

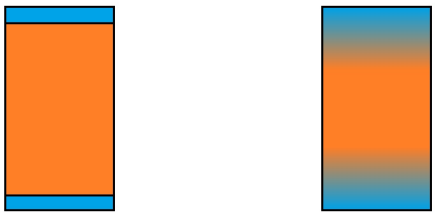

(a) Classic sandwich (b) FG sandwich

Figure 2: Schematization of the difference between a classic sandwich and a functoinally graded sandwich panel, which has a gradual transition from stiff to compliant material.

The objective of this work is to design, manufacture, and model the mechanical behavior of functionally graded sandwich beams, in order to obtain optimized combinations of stiffness and damping. For this purpose, the viscoelastic mechanical properties of the base 3-D printed materials (*i.e.* VeroCyan and TangoBlack+) have been obtained experimentally using various

techniques. Three different designs of graded sandwich structures have been proposed and modeled: linear graded face sheets, quadratic graded face sheets and quadratic graded core.

2 Material Properties: Theory

The base materials used are photopolymers, ranging from rigid ABS-like (VeroCyan) to a rubber-like elastomer (TangoBlack+). Therefore, the viscoelastic dynamic behavior of these materials has to be characterized. This section covers the theory necessary to understand both the mechanical behavior of the studied materials and the tests performed to obtain these properties (explained in the following section).

2.1 Behavior under periodic loading

Assuming a sinusoidal strain input of the form $\epsilon(t) = \epsilon_0 e^{i\omega t}$, we can define the dynamic frequency dependent mechanical properties of a material using a one-sided Fourier sine and cosine transform as follows:

$$E'(\omega) \equiv E_\infty + \omega \int_0^\infty \hat{E}(t') \sin \omega t' dt' \tag{1}$$

$$E''(\omega) \equiv \omega \int_0^\infty \hat{E}(t') \cos \omega t' dt' \tag{2}$$

$$\sigma(t) = E^*(\omega)\epsilon(t) = (E'(\omega) + iE''(\omega))\epsilon(t) \tag{3}$$

where $E(t) \equiv \hat{E}(t) + E_\infty$, E_∞ is the equilibrium modulus (or long term modulus) and E^* is the complex modulus. E' is the storage modulus (component of the stress-strain ratio in phase with the strain) and E'' is the loss modulus (component at 90° with the strain). Then, loss tangent can be defined as:

$$\tan \delta(\omega) \equiv \frac{E''(\omega)}{E'(\omega)} \tag{4}$$

which is the phase difference between the stress and the strain and represents the loss or damping of the material.

For a linear viscoelastic material, the stress-strain relation under dynamic oscillatory loading forms a curve with an elliptic shape called the hysteresis loop [9], as shown in figure 3:

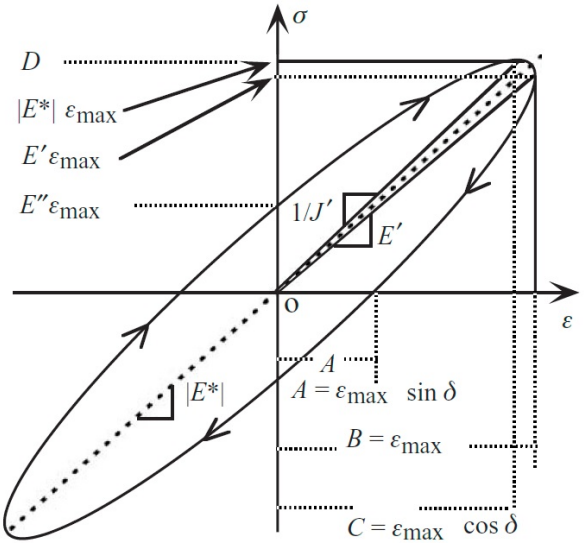

Figure 3: Stress-strain curve for a linear viscoelastic material undergoing a dynamic sinusoidal loading [9].

Using the expressions described in figure 3 the loss tangent can be obtained from the dimensions of the ellipse as $\tan(\delta) = A/C$, where A is the strain when stress is zero and C is the strain at maximum stress. The area enclosed by the stress-strain hysteresis loop represents the energy dissipated per unit volume in one cycle. Taking a quarter cycle (because in a full cycle the stored energy is equal to zero), the loss tangent can be obtained as:

$$\frac{W_l}{W_s} = \frac{\pi}{2}\tan(\delta) \tag{5}$$

where W_l is the loss (or dissipated) energy in a quarter cycle and W_s is the stored energy in a quarter cycle. Thus, the loss tangent represents a ratio of the mechanical energy dissipated over the stored energy.

2.2 Relaxation

Stress relaxation is the progressive decrease of stress when a constant strain step ϵ_0 is applied and held. The relation between stress and strain is called the relaxation modulus and for linear viscoelastic materials it only depends on time (it does not depend on the strain level):

$$E(t) = \frac{\sigma(t)}{\epsilon_0} \tag{6}$$

The model used to represent the behavior of the stress relaxation is the standard linear solid:

$$E(t) = E_\infty + \hat{E}e^{-t/\tau_r} \tag{7}$$

where τ_r is the relaxation time (*i.e.* the time it takes to completely relax to the value E_e). However, a model with a single exponential does not represent the behavior of real materials accurately enough. Therefore, a much realistic model can be defined using a sum of exponentials to represent the relaxation modulus:

$$E(t) = E_\infty + \sum_{n=0}^{N} E_n^{-t/\tau_{rn}} \tag{8}$$

this sum of exponentials is known as Prony series and is one of the techniques used in this work to characterize the mechanical properties of the materials. In equation 8 the series is defined for the relaxation modulus, but depending on the strain applied a Prony series can also be defined for the shear modulus $G(t)$ or the bulk modulus $K(t)$.

3 Experimental Methods and Results

In this section the methods used to experimentally characterize the mechanical behavior of materials are detailed. Given the variability obtained in the results, the materials have been tested in three different methodologies in order to obtain a wider set of data and add consistency of the results: (1) tension-compression cyclic loading, (2) stress relaxation tests and (3) bouncing tests. Initially, only the two "pure" materials (*i.e.* VeroCyan and TangoBlack+) were tested and the properties of the blends were assumed to be linearly proportional to the volume fraction of the constituents. However, in more advanced stages of this work, samples of blended materials were also tested to validate the hypothesis.

3.1 Tension-compression cyclic loading

As explained in section 2, the stress-strain relation for a viscoelastic material undergoing a cyclic sinusoidal displacement forms a hysteresis loop with an elliptic shape. From the dimensions of this ellipse the value of complex modulus

E^* can be fully determined (norm and phase) for a given angular frequency ω, thus giving information of the stiffness and the damping of the material at this given frequency.

Four tensile samples of each of the base materials were printed with the Connex3. Since the mechanical properties can present variability depending on the direction of printing and position on the tray [10, 11], the four samples of each material were printed in different orientations as shown in figure 4, to account for any possible anisotropy:

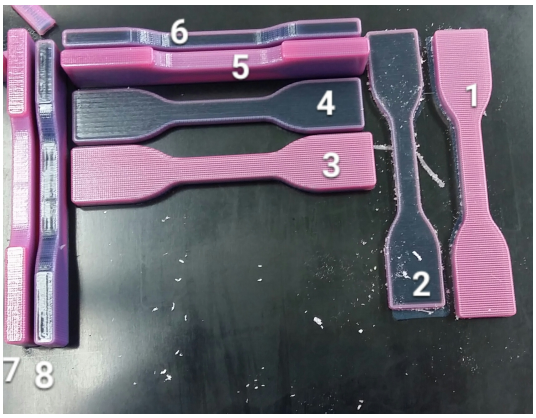

Figure 4: Tensile samples printed (1-8) in their position on the tray. The printing direction of the jets relative to the image is from left to right.

The samples were tested in an Instron mechanical press under a displacement control, following sinusoidal cycles at 1% and 2% strain. The VeroCyan samples were successfully tested and meaningful data was obtained. However, the TangoBlack+ samples were found to be three orders of magnitude more compliant and the available tension grips and load cell weren't able to measure such small forces, so no useful data could be obtained from these set of tests for this material. Barclift *et al.* [11] found that the direction in which the samples were printed implied variation in the mechanical properties, but without statistical difference. Agreeing with their work, the VeroCyan samples presented a slight variation on stiffness depending on the direction but the difference was not considered sufficient and thereby the materials are considered isotropic.

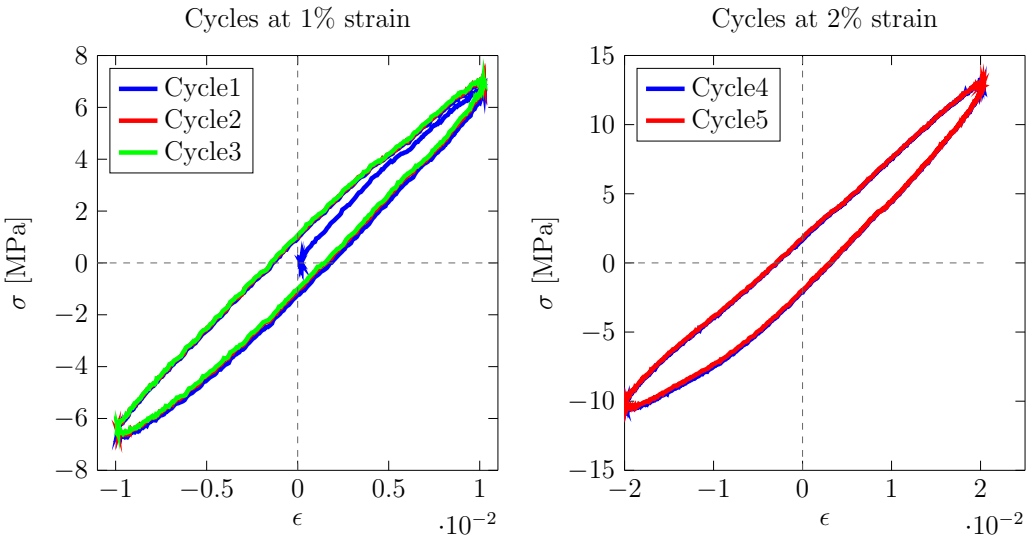

Figure 5: Tension-compression tests for sample 5 (VeroCyan) at 1% strain (left) and 2% strain (right) for a strain rate $\dot{\epsilon} = 0.02$mm/s.

As shown in figure 5, the experimental hysteresis loops plots are elliptical as expected. In the case of the 2% strain cycles the shape of the curve is less uniform, especially in compression. This is due to the appearance of buckling on the compression part of the cycles.

3.2 Stress relaxation tests

Stress relaxation tests were carried out for both VeroCyan and TangoBlack samples as well as for two different intermediate blends: DM95 and DM50. In the case of pure TangoBlack and the two mixed materials the samples were cylindrical (20mm diameter and 40mm height) and were loaded in compression. For VeroCyan, the same tensile samples used for tension-compression cycling were used for stress relaxation tests in tension. In order to simulate a strain step, the samples were loaded at a high strain rate ($\dot{\epsilon} = 0.5$mm/s), so that it took less than 2 seconds to reach the constant strain ϵ_0=2%.

The evolution of the relaxation modulus over time was obtained from the tests as shown in equation 6. Then the data was exported to Matlab and treated using two different methodologies.

3.2.1 Abaqus simulations

One of the input options for viscoelastic material properties in Abaqus is directly entering the coefficients of a Prony series from a relaxation or a creep test. However, the Prony series data for Abaqus needs to be a function of the normalized shear modulus $g(t) = G(t)/G_0$, instead of the relaxation modulus $E(t)$. Therefore, since the experimental data was obtained from a tension (or compression) test, it needs to be converted into shear. To do that, the bulk modulus $K(t)$ was assumed to be constant, which is quite realistic for materials with high Poisson's ratio ν, and once the initial bulk modulus is calculated the shear modulus is obtained for every data point as follows:

$$K = \frac{E_0}{3(1-2\nu_0)} \tag{9}$$

$$G(t) = \frac{3KE(t)}{9K - E(t)} \tag{10}$$

where E_0 is the initial relaxation modulus and ν_0 is the initial Poisson's ratio. The values for Poisson's ratio were set to 0.37 for VeroCyan and 0.48 for TangoBlack+ and the two mixed materials. Once the normalized shear modulus data is obtained, it is fitted into a sum of exponentials with the form of a Prony series with $N = 4$ viscoelastic branches (four exponential terms). Finally a steady-state simulation is carried out in Abaqus using a frequency of $f = 0.0075$Hz, which is the same used in the experimental tension-compression tests.

3.2.2 Fourier transform

The storage modulus and tangent modulus as a function of time can be obtained from the relaxation modulus using a one-sided Fourier transform as shown in equations 1 and 2. Thus, fitting the relaxation modulus to a Prony series with $N = 4$ viscoelastic branches as in equation 8, E' and E'' can be obtained for any frequency ω. Therefore the complex modulus and loss tangent can be also obtained following equations 3 and 4.

3.3 Bouncing tests

In order to expand the dataset of the damping of the materials, a bouncing test was designed and implemented. Solid spheres (20mm diameter) of the same four materials as for the relaxation tests were printed and tested. The tests consisted in dropping the spheres inside an acrylic (transparent) tube from a height of 4 feet and optically measure the height of their first bounce. Five trials were carried out for every material and the results were averaged to reduce the variability of the obtained value.

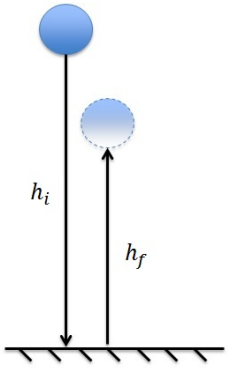

Figure 6: Schematization of the bouncing test, where h_i is the height from which the spheres are dropped and h_f is the height of the first bounce.

When a sphere impacts with the ground, it first deforms (flattens) and then comes back to its original configuration, which can be assimilated as half of the hysteresis loop. This means that the dissipated energy in one bounce is twice as much as the energy dissipated in a quarter cycle, but the initially stored energy is the same (in this case the initial gravitational potential energy). Accounting for the dissipated energy as the different of potential energy between the initial height and the height after the first bounce, and the relation in equation 5 for a quarter cycle, the loss tangent can be obtained as:

$$\frac{W_l}{W_s}\Big|_{1/4cycle} = \frac{E_l/2}{E_s}\Big|_{1/2cycle} \tag{11}$$

$$\tan(\delta) = \frac{h_i - h_f}{\pi h_i} \tag{12}$$

where E_l and E_s are the dissipated and the stored energy in a bounce respectively, and h_i and h_f are the initial height and the first bounce height respectively (as defined in figure 6).

3.4 Results

In this section the summary of the results obtained with the techniques explained above are summarized. Table 1 shows the averaged results for all the tests for the two base materials:

Table 1: Averages tests results for the complex modulus and the loss tangent.

	Tens-Comp		Simulation		Fourier		Bouncing	
Material	TB+	VC	TB+	VC	TB+	VC	TB+	VC
$\|E^*\|$[MPa]	0.367	717.9	0.367	484.4	0.366	502.21	-	-
$\tan(\delta)$	0.121	0.157	0.0344	0.127	0.0353	0.140	0.315	0.234

There is no stiffness data for the bouncing tests in table 1 because this technique only gives an approximation of the energy dissipation. Similarly, even though the TangoBlack+ tensile samples couldn't be tested in tension-compression cycling, the cylindrical samples from the stress relaxation tests were also tested in a compressive cycle under a sinusoidal displacement. This allowed to obtain a curve almost equivalent to the lower half of the hysteresis loop (not exactly equal to half of the loop because it is loaded in compression without any positive residual strain).

A surprising result is that all the methods except the bouncing tests give a very low damping for TangoBlack+ (even lower than for VeroCyan), which does not seem to be possible. For this reason, the trusted values of damping are the ones obtained with the bouncing tests. However, it is believed that the results obtained are not extremely realistic (especially for high damping materials such as TangoBlack+) for two reasons: (1) because it doesn't take into account the air friction inside the tube, which causes a piston effect that might not be negligible and (2) because equation figure 12 has a limit at $1/\pi$ while a material that dissipates all the energy should have loss tangent equal to 1. In contrast, the stiffness values obtained for TangoBlack+ are very consistent. In the case of VeroCyan, all the results seem reasonable but have a significant variability.

In conclusion, the definitive values of stiffness and loss tangent were taken as follows: $E = 600$GPa and $\tan(\delta) = 0.234$ for VeroCyan and $E = 0.367$GPa and $\tan(\delta) = 0.315$ for TangoBlack+.

4 Design of the graded structures

When a sandwich beam has to be loaded in bending the face sheets are placed on the top and the bottom layers of the sandwich, as shown in figure 1, carrying the biggest normal stresses. Thus, the gradual variation of material composition has to be in the vertical direction (y axis).

One of the main problems of the materials obtained from the Objet Connex3 is that they have a very similar density: 1175kg/m^3 for VeroCyan and 1125kg/m^3 for TangoBlack+. This means that one of the main advantages of the sandwich panels, light weight, cannot be a design parameter because there is practically not a weight reduction if using one material or the other.

Three different graded designs have been proposed: (1) pure core and linear gradation in the face sheets, (2) pure core and quadratic gradation in the face sheets and (3) pure face sheets and quadratic gradation in the core. The local composition has been defined as a function of the vertical coordinate y and two parameters m_s and m_c defined as pure stiff material or pure compliant material respectively (equal to one if the volume fraction is calculated for that material and equal to zero if calculated for the other material). Therefore, the local volume fraction for a specific location y will be a weighted function of m_s and m_c. Equations 13 and 14 express the evolution of composition in y for a purely linear graded sandwich and a purely quadratic graded structures respectively:

$$\phi_l(y) = m_c + \frac{m_s - m_c}{h/2}|y| \tag{13}$$

$$\phi_q(y) = m_c + \frac{m_s - m_c}{(h/2)^2}y^2 \tag{14}$$

where h is the thickness of the entire structure. Integrating each of these equations over the entire section (or half of it, due to symmetry along the longitudinal axis), the overall volume fraction of the constituents in the entire section can be obtained for the linear and the quadratic gradations:

$$\Phi_l = \frac{2}{h}\int_0^{h/2} \phi_l(y)dy = \frac{m_s + m_c}{2} \tag{15}$$

$$\Phi_q = \frac{2}{h}\int_0^{h/2} \phi_q(y)dy = \frac{m_s + 2m_c}{3} \tag{16}$$

The result from equations 15 and 16 show that depending on the model of gradation, a sandwich with a section entirely graded has a different content of stiff material and compliant material: the linear has a 50-50% stiff-compliant material ratio whereas the quadratic has 33-66%. In order to compare the graded designs with each other and with the classic sandwich, they need to have the same overall volume content of the two constituents. To achieve that, a geometric parameter is also introduced to every design (h', h'' and h'''respectively) as shown in figure 7 to define the frontier between the pure material and the functionally graded zone:

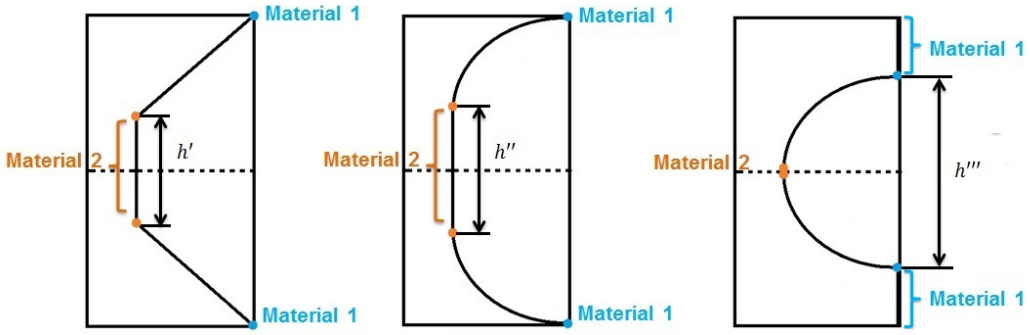

Figure 7: Schematization of the materials distribution in the graded designs proposed. From left to right: linear face sheets, quadratic face sheets and quadratic core.

Using the frontier parameters introduced in figure 7, the overall volume fraction for each of the designs is, respectively:

$$\Phi_{lf} = \frac{1}{h}\left[m_c h' + \frac{m_s + m_c}{2}(h - h')\right] \tag{17}$$

$$\Phi_{qf} = \frac{1}{h}\left[m_c h'' + \frac{m_s + 2m_c}{3}(h - h'')\right] \tag{18}$$

$$\Phi_{qc} = \frac{1}{h}\left[\frac{m_s + 2m_c}{3}h''' + m_s(h - h''')\right] \tag{19}$$

where h is the total thickness of the section. These three equations can be particularized, for example, for the stiff material, and then the frontier parameters can be obtained as a function of the volume fraction of stiff material, which allows defining h', h'' and h''' for a given overall material composition:

$$h' = h(1 - 2\Phi_{lf,s}) \tag{20}$$

$$h'' = h(1 - 3\Phi_{qf,s}) \tag{21}$$

$$h''' = \frac{2}{3}h(1 - \Phi_{qc,s}) \tag{22}$$

5 Model of the mechanical response

The mechanical properties of the three graded sandwich structures and the classic sandwich have been studied in 3-point bending (see fig 8):

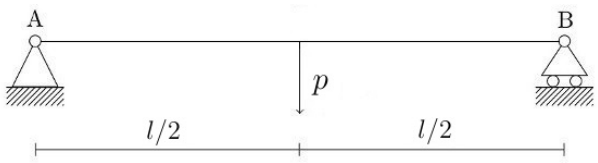

Figure 8: Diagram of a beam loaded under 3-point bending boundary conditions.

Using the Casitgliano's theorem the maximum deflection δ (which will be in the central section, where the load p is applied) on a beam can be obtained as a function of the load p as:

$$\delta = \int_0^l \left(\frac{T(x)}{GA} \frac{\partial T}{\partial p} + \frac{M(x)}{EI} \frac{\partial M}{\partial p} \right) dx \tag{23}$$

where T is the shear force, A is the cross sectional area, M is the bending moment, I is the area moment of inertia and x is the longitudinal coordinate. For a general beam and the particular case of 3-point bending, the bending stiffness of the beam can then be obtained independently of the load p as:

$$k = \frac{p}{\delta} = \frac{1}{\frac{l}{4GA} + \frac{l^3}{48EI}} \tag{24}$$

For a classic sandwich this calculation is quite straight forward, but it is not trivial for a functionally graded structure because the modulus of elasticity E and the shear modulus G are not constant across the section. To address this, first the Voigt model is used to assess the properties of a layer of material: if a layer is made of two material constituents m_s and m_c, the Young's modulus is proportional to the volume fraction according to:

$$E_{tot} = (E_s - E_c)\phi_s + E_c \tag{25}$$

this equation being also valid for the Poisson's ratio and the density. Thus, the shear modulus for any layer can be obtained from the Young's modulus and the Poisson's ratio as $G_{tot} = E_{tot}/2(1+\nu)$. In equation 24 the shear modulus is weighted by the cross sectional area, therefore GA is assumed to be the area times the shear modulus calculated with the overall volume fraction in the sandwich structure.

In the case of the bending rigidity EI, the stiffness of the material is more weighted further from the horizontal axis. For a graded material, the stiffness is a function of the volume fraction in every layer, hence, the overall bending rigidity of the structure depends on the grading function:

$$EI_{tot} = \int_A E(y)y^2 dA = b\int_Y E(y)y^2 dy \tag{26}$$

where b is the width of the section and $E(y)$ is the modulus of elasticity of the graded sandwich as a function of the vertical coordinate y.

5.1 Linear gradation model

For a linear graded sandwich structure as the shown in figure 7 and assuming a linear relation of the modulus of elasticity with the volume fraction as previously explained in this section, the stiffness distribution is:

$$E_{lf}(y) = \begin{cases} E_c - \frac{E_s - E_c}{\frac{h-h'}{2}}\left(y + \frac{h'}{2}\right) & -\frac{h}{2} \leqslant y < -\frac{h'}{2} \\ E_c & -\frac{h'}{2} \leqslant y \leqslant \frac{h'}{2} \\ E_c + \frac{E_s - E_c}{\frac{h-h'}{2}}\left(y - \frac{h'}{2}\right) & \frac{h'}{2} < y \leqslant \frac{h}{2} \end{cases} \tag{27}$$

now this piecewise function $E_{lf}(y)$ is integrated as shown in equation 26 over the entire section and the bending rigidity is obtained:

$$EI_{tot} = \frac{b}{12}\left[E_c h^3 + \frac{3}{4}\frac{E_s - E_c}{h - h'}\left(h^4 - h'^4\right) - \frac{E_s - E_c}{h - h'}h'\left(h^3 - h'^3\right)\right] \tag{28}$$

From equation 20, the parameter h' can be determined for the desired volume fraction of constituents and then the bending rigidity EI_{tot} of the entire linear graded structure is obtained for a given cross sectional dimensions b and h. Finally, the bending stiffness k is calculated as in equation 24.

5.2 Quadratic gradation model

The quadratic graded model is broken into two different designs, as shown in figure 7: a design with pure stiff face sheets and graded core and a design with a pure compliant core and graded face sheets. The reason why the quadratic model is separated but not the linear is because with the linear model proposed it is possible to obtain graded sandwich structures ranging from 0% to 50% of stiff material. However, with the analogous quadratic design (quadratic

face sheets and pure core) it is only possible to obtain combinations from 0% to 33% of stiff material. Hence, in order to have a study where the classic sandwich, a linear graded design and a quadratic graded design are compared in a wider range of material compositions ($\Phi_{stiff} \in [0, 0.5]$), the two types of quadratic gradation design need to coexist.

5.2.1 Quadratic graded face sheets and pure compliant core

This design is valid for volume fractions of stiff material under 1/3. The distribution of the stiffness of the mixed material for this model is:

$$E_{qf}(y) = \begin{cases} E_c + \frac{E_s - E_c}{\left(\frac{h-h''}{2}\right)^2}\left(y + \frac{h''}{2}\right) & -\frac{h}{2} \leqslant y < -\frac{h''}{2} \\ E_c & -\frac{h''}{2} \leqslant y \leqslant \frac{h''}{2} \\ E_c + \frac{E_s - E_c}{\left(\frac{h-h''}{2}\right)^2}\left(y - \frac{h''}{2}\right)^2 & \frac{h''}{2} < y \leqslant \frac{h}{2} \end{cases} \tag{29}$$

now this piecewise function $E_{qf}(y)$ is integrated as shown in equation 26 over the entire section and the total bending rigidity is obtained as a function of the dimensions b, h and h'' :

$$EI_{tot} = \frac{b}{12}\left[E_c h^3 + \frac{E_s - E_c}{(h-h')^2}\left(h''^2\left(h^3 - h''^3\right) + \frac{3h''}{2}\left(h''^4 - h^4\right) + \frac{3}{5}\left(h^5 - h''^5\right)\right)\right] \tag{30}$$

5.2.2 Quadratic graded core and pure stiff face sheets

This design is valid for volume fractions of stiff material above 1/3. The distribution of the stiffness of the material for this model is:

$$E_{qc}(y) = \begin{cases} E_c & -\frac{h}{2} \leqslant y < -\frac{h''}{2} \\ E_c + \frac{E_s - E_c}{(h'/2)^2} y^2 & -\frac{h''}{2} \leqslant y \leqslant \frac{h''}{2} \\ E_c & \frac{h''}{2} < y \leqslant \frac{h}{2} \end{cases} \tag{31}$$

now this piecewise function $E_{qc}(y)$ is integrated as shown in equation 26 over the entire section and the total bending rigidity is obtained as a function of the dimensions b, h and h''' :

$$EI_{tot} = \frac{b}{12}\left[E_s h^3 + 2\frac{E_c - E_s}{5} h'''^3\right] \tag{32}$$

5.3 Results

As explained in sections 2 and 3 both materials used exhibit a viscoelastic behavior, although the model only contains the modulus of elasticity. However, the modulus of elasticity E can be interchanged in the model by the complex modulus E^*, which has the same norm but also a phase δ (as detailed in section 2). Introducing the complex modulus of both materials will transform the bending rigidity, the shear rigidity and the bending stiffness into complex numbers. Therefore, the bending stiffness k of the structure will also contain information of the damping of the entire sandwich structure.

The bending stiffness k was computed (as in equation 24) for a classic sandwich model, the linear graded sandwich model and the quadratic graded sandwich model for compositions of stiff material ranging from 0% to 50%. The stiff material from the model corresponds to VeroCyan and the compliant material corresponds to TangoBlack+. Figure 9 shows the results of stiffness obtained from the model for the classic sandwich, linear graded and quadratic graded sandwich structure:

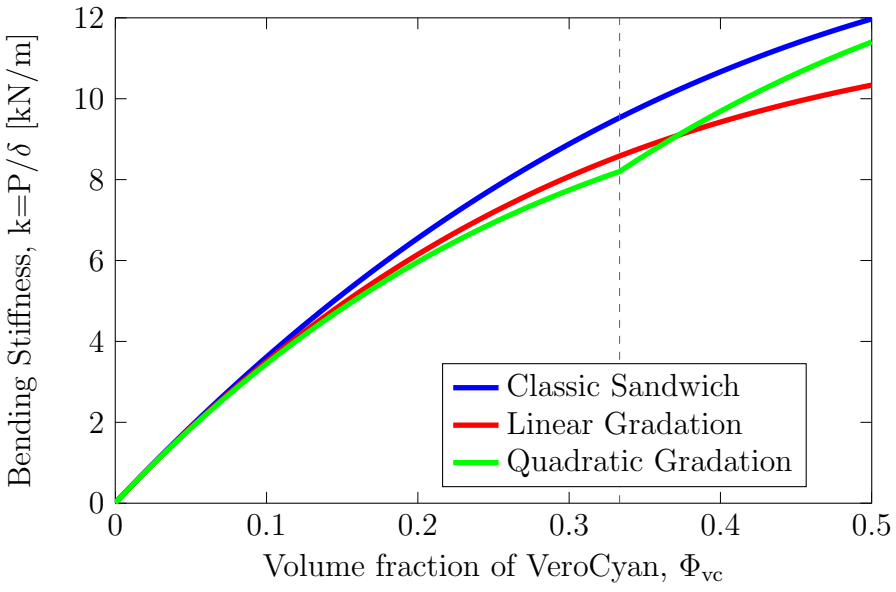

Figure 9: Bending stiffness as a function of the volume fraction of VeroCyan for all models studied.

where the vertical dashed line symbolizes the change of model for the quadratic graded structure: from pure TangoBlack+ core and quadratic graded

face sheets (for $\Phi_{vc} < 1/3$) to quadratic graded core and pure VeroCyan face sheets (for $\Phi_{vc} > 1/3$).

The most important conclusion that can be drawn from this results is that for designs with predomination of TangoBlack+, approximately $\Phi_{vc} < 0.15$, the three models exhibit very low difference in stiffness. This is a satisfactory result because usually sandwich panels have a very low volumetric content of stiff material, which means that for a realistic graded sandwich structure there is not an important sacrifice in stiffness in comparison with a classic sandwich structure. On the other hand, the damping results are surprisingly unsatisfactory. As shown in figure 10, the three models are practically superimposed and the value of $\tan(\delta)$ is equal to the one of pure VeroCyan:

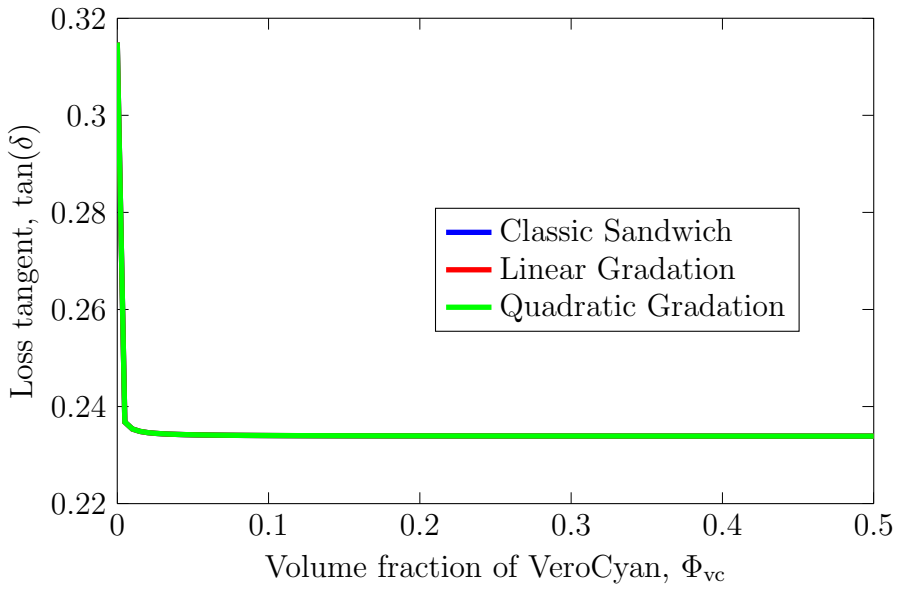

Figure 10: Loss tangent as a function of the volume fraction of VeroCyan for all models studied.

These results are probably due to the difference in the ratio of the stiffnesses of the two materials when compared to the ratio of the damping. The stiffness of VeroCyan is 2000 times greater, but the loss tangent of TangoBlack+ is not even 1.5 times greater. Consequently, when making weighted sums of E^*_{vc} and E^*_{tb} as in equations 28, 30 and 32 the difference in magnitude plays a much more important role than the difference in phase.

6 Manufacturing: voxel printing

The Stratasys Objet260 Connex 3 machine can print a using default palette of different blends of the base materials VeroCyan and TangoBlack+, but there are not enough to generate a realistic functionally graded structure. In order to achieve that, the Voxel Printing extension of the machine software was used.

A voxel is a unit of graphic information that defines a 3D point in space: it is the 3D analogous of a pixel. The idea behind Voxel Printing is that the model to be printed has to be previously broken up, at a microscopic scale, into voxels and then assign one of the base materials (in our case VeroCyan or TangoBlack+) to be printed in every voxel. Thus, the combination of thousands of voxels of the base materials result in a digital material with the desired composition and mechanical properties (see figure 11).

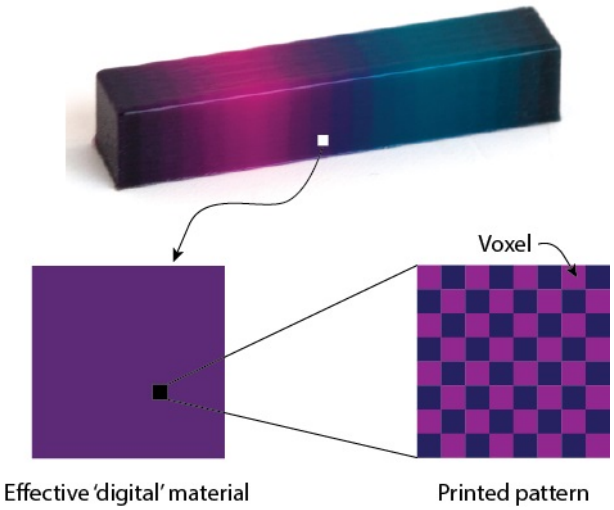

Figure 11: Explicative diagram of the formation of digital materials from printed voxels of the base materials.

The Voxel Printing feature works by layers. The model to be printed has first to be sliced into layers with a 30μm thickness, which is the layer thickness that the machine is able to print. Every layer needs to have an associated pattern (a bitmap) for every material, which establish what material has to be printed in every voxel of every layer of the structure. Thus, a sandwich beam with dimensions b x h x l will have $N = h/0.03$ layers, and N bitmaps for every base material used.

This process of creation of the stack of bitmaps was implemented using a Matlab routine. First, a volume fraction is assigned to every layer discretizing according to the desired functionally graded design (defined as in the previous sections). For the first material, a black image is created for the first layer of the model with the dimensions of the beam (bxl) converted to pixels: the in-plane printing resolution of the machine is 600($xaxis$)x300(y axis)dpi, so every pixel of the bitmap will represent a rectangle of dimensions $\frac{1}{600}$x$\frac{1}{300}$inch. As an example, a stack of bitmaps with twice as much pixels in x direction than in y will be physically printed as a square. Then, according to the volume fraction corresponding to the layer, a certain number of pixels (randomly distributed) are changed from black to white meaning that the material in question is assigned to that voxel:

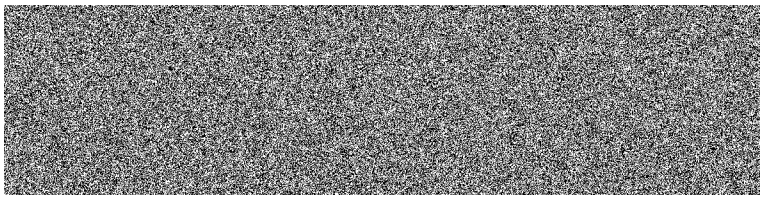

Figure 12: Bitmap of a layer with a 50%-50% composition for a sandwich of dimensions $b = 25$mm and $l = 50$mm.

For the same layer, a complementary bitmap is generated for the other material assigning this second material to the voxels that were empty: only one material can be assigned to a voxel, but every voxel mus have a material assigned. Therefore, repeating this process for every layer and with the corresponding volume fraction, a stack of bitmaps is generated for every material. These stacks of bitmaps contain the information of what material is going to be printed in every microscopic voxel of the structure, thus allowing for a deep level of personalization of the design of the structures to be manufactured and their macroscopic properties.

7 Conclusions

In this work, an approach for the design, manufacturing via ploy jet multi material 3D printing and modeling of the mechanical properties of functionally graded sandwich panels has been proposed.

Firstly, the mechanical viscoelastic properties of the base materials used were studied and tested using a variety of techniques, since the available data from the manufacturer is insufficient. The results obtained present a high variability and there is not a full consistency between methods. Therefore, the real modulus of elasticity or the loss tangent of the materials could slightly differ from the values assumed in this work and later used for the modeling of the mechanical response of the sandwich structure. However, in this work a variety of methodologies have been detailed and implemented, which can be useful for future investigations on the characterization of the viscoelastic properties of the Connex3 materials.

Secondly, functionally graded sandwich structures have been successfully designed and modeled using a linear and quadratic gradation. The model results show that the stiffest structure is the classic sandwich, as expected, because it has all the stiff material concentrated purely on the edges away from the neutral bending axis. For compositions under 15% of stiff material (VeroCyan) the linear graded and the quadratic graded structures show practically the same stiffness as the classic sandwich. This is a satisfactory result because it means that a gradual transition from stiff to compliant barely results in a sacrifice in stiffness of the sandwich structure.

Instead, it has been found that for compositions with any VeroCyan, the damping of the structure is the same as the damping of pure VeroCyan. We believe that this is due to the fact that VeroCyan has been found to be dramatically stiffer than TnagoBlack+ (2000 times stiffer), while the loss tangent of TangoBlack+ is only 1.35 times greater: $\frac{E_s}{E_c} >> \frac{\tan\delta_c}{\tan\delta_s}$. The introduction of 3D printable materials with a wider range of damping would possibly allow higher variations on the energy dissipation of the sandwich panels, hence, the introduction of damping as a design parameter too.

Nonetheless, as in other works on graded materials [6], the model is based in the Voigt assumption that the modulus of elasticity scales linearly with the volumetric composition of the two basic constituents. As a purpose for future work, this assumption should be validated experimentally for the case of 3D printed materials, testing different blends of known composition to determine the function that relates the stiffness and the composition of the materials.

In addition to that, the code to manufacture graded sandwich panels by voxel printing has been implemented. Due to technical difficulties experienced with the Connex3 we were not able to print and test actual sandwich samples, but this is one of the main future research lines to come after this project. Thereby, there will be experimental data to contrast the results obtained with the analytical model proposed.

Finally, we plan on investigating the effects that functional gradation of composition has on the strength of the structure. We believe that it will improve the strength of the interface, thus increasing the resistance to crack propagation and, consequently, delamination. Once the strength of the interface for different functionally graded sandwich panels is better characterized, structures with optimal combinations of stiffness and strength can be studied using topology optimization algorithms.

8 References

[1] A. Johnson and G. Sims. Mechanical properties and design of sandwich materials. *Composites*, pp. 312-328 1986.

[2] L. J. Gibson and M. F. Ashby. Cellular solids. *Cambridge University Press*, 2nd edition (1997). ISBN 0 521 49911 9.

[3] M. F. Ashby, A. Evans, N. A. Fleck, L. J. Gibson, J. W. Hutchingson and H. N. Wadley. Metal Foams: a Design Guide. *Butterworth Heinemann* (2000). ISBN 0 7506 7219 6.

[4] V. Crupi, G. Epasto and E. Guglielmino. Low-velocity impact strength of sandwich materials. *Journal of Sandwich Structures and Materials*, pp. 1-18 2010.

[5] W. J. Cantwell and P. Davies. A Study of Skin-Core Adhesion in Glass Fibre Reinforced Sandwich Materials. *Applied Composite Materials*, vol. 3, pp. 407-420 1996.

[6] Z. Su, G. Jin, Y. Wang and X. Ye. A general Fourier formulation for vibration analysis of functionally graded sandwich beams with arbitrary boundary condition and resting on elastic foundations. *Acta Mechanica*, vol. 227, p. 1493–1514 2016.

[7] B. Koohbor and A. Kidane. Design optimization of continuously and discretely graded foam materials for efficient energy absorption. *Materials and Design*, vol. 102, pp. 151-161 2016.

[8] P. Tossapanon and N. Wattanasakulpong. Stability and free vibration of functionally graded sandwich beams resting on two-parameter elastic foundation. *Composite Structures*, vol. 142, pp. 215-225 2016.

[9] R. Lakes. Viscoelastic Materials. *Cambridge University Press* (2009). ISBN 0 521 88568 3.

[10] J. Mueller, K. Shea and C. Daraio. Mechanical properties of parts fabricated with inkjet 3D printing through efficient experimental design. *Materials and Design*,vol. 86 902-912 (2015).

[11] M. W. Barclift and C. B. Williams, Examining variability in the mechanical properties of parts manufactured via polyjet direct 3D printing. *International Solid Freeform Fabrication Symposium*, August 6-8 2012.